J Neurophysiol
88: 1743–1752, 2002; 10.1152/jn.00322.2002.

Quantitative Analysis of High-Frequency Oscillations (80–500 Hz) Recorded in Human Epileptic Hippocampus and Entorhinal Cortex

RICHARD J. STABA,[1] CHARLES L. WILSON,[2,4] ANATOL BRAGIN,[2,4] ITZHAK FRIED,[3,4] AND JEROME ENGEL, JR[1,2,4]

Departments of [1]Neurobiology, [2]Neurology, and [3]Neurosurgery and [4]The Brain Research Institute, David Geffen School of Medicine at UCLA, Los Angeles, California 90095

Received 1 May 2002; accepted in final form 25 June 2002

Staba, Richard J., Charles L. Wilson, Anatol Bragin, Itzhak Fried, and Jerome Engel, Jr. Quantitative analysis of high-frequency oscillations (80–500 Hz) recorded in human epileptic hippocampus and entorhinal cortex. *J Neurophysiol* 88: 1743–1752, 2002; 10.1152/jn.00322.2002. High-frequency oscillations (100–200 Hz), termed ripples, have been identified in hippocampal (Hip) and entorhinal cortical (EC) areas of rodents and humans. In contrast, higher-frequency oscillations (250–500 Hz), termed fast ripples (FR), have been described in seizure-generating limbic areas of rodents made epileptic by intrahippocampal injection of kainic acid and observed in humans ipsilateral to areas of seizure initiation. However, quantitative studies supporting the existence of two spectrally distinct oscillatory events have not been carried out in humans nor has the preferential appearance of FR within seizure generating areas received statistical evaluation based on analysis of a large sample of oscillatory events. Interictal oscillations within the bandwidth of 80–500 Hz were detected in Hip and EC areas of patients with mesial temporal lobe epilepsy using wideband EEG recorded during non-rapid eye-movement sleep from chronically implanted depth electrodes. Power spectral analysis showed that oscillations detected from Hip and EC areas were composed of two spectrally distinct groups. The lower-frequency ripple group was defined by a frequency of 96 ± 14 Hz (median ± width), while the higher-frequency FR group had a frequency of 262 ± 59 Hz. FR oscillations were significantly shorter in duration compared with ripple oscillations ($P < 0.0001$). In regard to the occurrence of FR and ripples in epileptic Hip and EC, the mean ratio of the number of FR to ripples generated in areas ipsilateral to seizure onset was significantly higher compared with the mean ratio of FR to ripple generation from contralateral areas ($P = 0.008$). Furthermore, sites ipsilateral to seizure onset with hippocampal atrophy had significantly higher ratios compared with sites contralateral to both seizure onset and hippocampal atrophy ($P = 0.001$). These data provide compelling quantitative and statistical evidence for the existence of two spectrally distinct groups of limbic oscillations that have frequency and duration characteristics similar to those previously described in epileptic rat and human Hip and EC. The strong association between FR and regions of seizure initiation supports the view that FR reflects pathological hypersynchronous events crucially associated with seizure genesis.

INTRODUCTION

Increasing interest surrounds the investigation of fast oscillations (>80 Hz) and their putative functional role in neural processes. Studies have shown that oscillations within the range of 100 to 200 Hz, termed "ripples," are present in non-primate hippocampus (Hip) and entorhinal cortex (EC) (Buzsaki et al. 1992; Suzuki and Smith 1988). Ripple oscillations have also been recorded in neocortical areas of rodents (Kandel and Buzsaki 1997) and cats (Grenier et al. 2001). The discrete nature of these events, possessing durations between 25 and 75 ms (Chrobak and Buzsaki 1996), and the variation of their occurrence across sleep/waking states have led some to suggest that ripples may be involved in hippocampal and neocortical wide-area networks associated with memory processing (Buzsaki 1998; Chrobak and Buzsaki 1996; Grenier et al. 2001; Siapas and Wilson 1998). In addition, somatosensory-evoked oscillations (>200 Hz) have been recorded in both rodent and human somatosensory cortex and presumably reflect the coordinated discharge of neurons involved with the processing of incoming sensory information (Curio et al. 1994; Jones and Barth 1999; Jones et al. 2000).

In contrast to the physiologically normal fast oscillatory activity described in the preceding text, high-frequency activity has been recorded preceding the onset of seizures in epileptic patients (Fisher et al. 1992) and the oscillatory characteristics of such activity described (Traub et al. 2001). Two recent papers have identified the presence of high-frequency oscillations in Hip and EC areas of patients with temporal lobe epilepsy (Bragin et al. 1999a,b). Results from these studies showed that ripple oscillations were present bilaterally and possessed many characteristics similar to those found in non-primates, although they were of a lower frequency (80–160 Hz) than non-primate ripples. In addition to ripples, Bragin and colleagues reported the occurrence of local field oscillations that displayed higher spectral frequencies compared with ripples and termed these oscillations "fast ripples" (FR; 250–500 Hz). This higher-frequency FR was limited to Hip and EC areas ipsilateral to the area of seizure onset in humans; this was consistent with the distribution of FR found only within sites adjacent to the kindled or excitotoxic lesion in epileptic rodents (Bragin et al. 1999a,b). These findings led to the proposal that FR were pathological and reflected the hypersynchronous discharge of locally interconnected principle neurons within epi-

Address for reprint requests: C. L. Wilson, 2155 Reed Neurological Research Center, 710 Westwood Plaza, UCLA School of Medicine, Los Angeles, CA 90095 (E-mail: clwilson@ucla.edu).

The costs of publication of this article were defrayed in part by the payment of page charges. The article must therefore be hereby marked "*advertisement*" in accordance with 18 U.S.C. Section 1734 solely to indicate this fact.

leptogenic areas capable of generating spontaneous seizures (Bragin et al. 1999b, 2000).

To further study human high-frequency oscillations (HFOs), we used a quantitative approach to address the following questions: first, is there statistical evidence supporting distinct modal oscillation frequencies within the frequency band of 80–500 Hz? Second, are there differences other than spectral frequency, e.g., duration, that distinguish these oscillatory events? Third, are some oscillations limited to seizure generating areas? To answer these questions, we studied HFOs in patients that were surgically implanted with depth electrodes required for localization of the epileptogenic region. Interictal wideband EEG was recorded from Hip and EC areas during overnight polysomnographic sleep studies. HFOs were detected from the sleep EEG recordings using automated techniques and each oscillation was characterized by its peak spectral frequency, duration, and proximity to seizure-generating areas.

METHODS

Subjects

Patients with medically intractable complex partial seizures were implanted with intracerebral clinical depth electrodes for localization of seizure onset area because noninvasive testing suggested focal seizure onsets but results were inconclusive. Prior to depth electrode implantation, patients gave their informed consent for participation in these research studies under the approval of the Internal Review Board of the UCLA Office for Protection of Research Subjects. Each patient was surgically implanted with 8–14 flexible polyurethane clinical depth electrodes stereotactically targeted to clinically relevant brain areas. EEG from these electrodes was continuously monitored on the telemetry unit for an average of 2 wk to find those brain areas in which spontaneous seizure activity began first (Fried et al. 1999). Patients in whom a seizure onset area could be localized became candidates for surgical removal of epileptogenic sites if resection of the area would not produce unacceptable neurological deficit.

Classification of recording site pathology

Identification of the epileptogenic region was based primarily on criteria from electrographic seizure recordings and neuroimaging (Engel 1996). Electrographic seizure onsets were recorded during the patient's depth electrode telemetry monitoring, and attending neurologists in the UCLA Seizure Disorders Center identified locations of seizure onset based on the recording of multiple seizure occurrences during the average 2 wk the patients spent in the hospital. In addition, attending neurologists evaluated each patient's fluorodeoxyglucose positron emission tomography scans (FDG-PET) for the presence or absence of areas of hypometabolism and its predominant location. A single neuroradiologist at UCLA evaluated every patient's magnetic resonance imaging (MRI) scans for the presence or absence of hippocampal atrophy and its location as part of the clinical evaluation. Recording sites were defined as "ipsilateral" if located in the same hemisphere as areas where seizure onsets occurred. All Hip and EC recording sites in patients ($n = 5$) with bilateral ictal onsets were considered ipsilateral to seizure onset. Recording sites were defined as "contralateral" if located in the hemisphere opposite to that of seizure initiation.

Electrodes and localization

Wideband EEG was recorded from bundles of nine platinum-iridium microwires, which were inserted through the lumen of the seven-contact clinical depth electrodes (1.25-mm diam), so that they extended 3–5 mm beyond the tip of the clinical electrode (Fried et al. 1999). Microwires were 40 μm in diameter with impedances ranging from 200 to 500 kΩ. Electrode tips were localized using the combined information from postimplant computed tomography (CT) scans co-registered with preimplant 1.5T MRI scans (Staba et al. 2002). The imaging software used (Brain Navigator, Grass-Telefactor, Philadelphia, PA) allowed for visualization and highlighting of electrode tip locations on CT that were automatically registered to the MRI scans. Anatomical boundaries were based on references of mesial temporal lobe anatomy by Duvernoy (1998) and Amaral and Insausti (1990). Only microwires verified as located in Hip and EC were used in analyses.

Sleep studies

Sleep studies were conducted on the hospital ward between the hours of 10 PM and 7 AM. A sleep record was acquired for each patient to correlate behavioral state with the concurrently recorded wideband EEG. The sleep record consisted of two electro-ocular channels to monitor eye movements, two electromyogram channels recording from the patient's chin to monitor muscle tone, and two EEG channels recording from International 10–20 System positions C_3 and C_4 (5–10 cm left and right, respectively, of midline at the skull vertex, depending on cranial size), each referenced to a contralateral auricle site, to monitor neocortical activity (Jasper 1958). The recording was staged according to the criteria of Rechtschaffen and Kales (1968) with stages labeled as waking (Aw), nonrapid eye-movement (NREM) sleep stages 1–4, and rapid eye-movement (REM) sleep. Episodes of Aw consisted of patients lying in bed and either sitting quietly with their eyes opened or engaged in quiet conversation with one of the investigators. Because the objective of our study was to characterize HFO activity in relation to areas of epileptogenicity, and the highest probability of HFO occurrence coincides with NREM episodes (Bragin et al. 1999a; Buzsaki et al. 1992; Suzuki and Smith 1988), the current paper is limited to the analysis of HFOs that occurred during episodes of NREM sleep i.e., stages 1–4.

High-frequency recordings and signal analysis

For each patient ($n = 25$), 16 channels of wideband (0.1 Hz to 5 kHz) interictal EEG were sampled from intracerebral microwires at 10 kHz with 12-bit precision using an R. C. Electronics EGAA acquisition system (Santa Barbara, CA). A 10-min NREM sleep-staged epoch of wideband EEG was visually inspected for the presence of HFO activity previously described within the non-primate and human entorhinal-hippocampus axis (Bragin et al. 1999b; Buzsaki et al. 1992; O'Keefe and Nadel 1978). Channels demonstrating oscillations with large amplitude sinusoid-like waves with frequencies between 80 and 500 Hz that were discernable above background EEG were selected for analysis.

Between three and five channels of EEG per patient were selected for detection and quantification of HFO events. The data analyzed for each patient included only episodes that were recorded during polysomnographically defined NREM sleep. Figure 1 illustrates the technique used to detect HFOs. Each channel of wideband EEG was digitally band-passed between 100 and 500 Hz (finite impulse response filter, rolloff, −33 dB/octave), and the root mean square (RMS; 3-ms sliding window) amplitude of the filtered signal was calculated (DataPac 2K2, Run Technologies, Mission Viejo, CA). Multiple filter cutoff frequencies and roll-off value combinations were tested to determine filter settings that would optimally pass the frequencies between 80 and 500 Hz. Successive RMS values with amplitudes >5 SDs above the mean amplitude of the RMS signal (i.e., mean amplitude calculated over the entire length of data file) longer than 6 ms in duration were detected and delimited by onset and offset boundary time markers as putative HFOs. Consecutive events sepa-

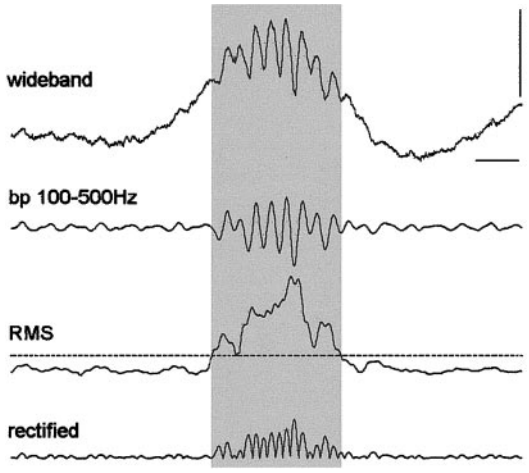

FIG. 1. Detection of spontaneous high-frequency oscillation (HFO) events from continuous wideband EEG recordings. *Top*: wideband EEG was band-pass filtered 100–500 Hz to identify high-frequency EEG events. The root mean square (RMS; 3-ms window) of the band-pass signal was calculated and used to detect HFO events. Successive RMS values greater than 5 SD above the overall mean RMS value (- - -, 5 SD threshold) and a minimum of 6 ms in duration were delimited by onset and offset boundaries (▨) and selected as putative HFO events. HFO events were subjected to the additional criterion of containing a minimum of 6 peaks that were greater than 3 SD above the mean value of the rectified band-pass signal (*bottom*). Calibration bars 0.5 mV and 5 ms.

rated by less than 10 ms were combined as one event. Events not having a minimum of 6 peaks (band-passed signal rectified above 0 μV) greater than 3 SD from the mean baseline signal were rejected. Each event was visually inspected to remove events that were contaminated by artifact, including movement, electronic, and other sources of signal noise. During development of this technique, it was found that it was effective in detecting greater than 84% of putative oscillatory events observable with visual EEG analysis.

Data analysis

For each HFO, duration was measured between onset and offset boundaries (Fig. 1, ▨) and peak spectral frequency was determined from fast Fourier transform (FFT)-based power spectral analysis. Power spectral histograms were calculated using 1,024-point FFT with zero padding to attain a frequency resolution of 9.7 Hz. To improve the spectral estimate for each HFO, the signal was band-passed filtered 80–500 Hz to attenuate power below 80 Hz associated with slow waves and power above 500 Hz associated with neuronal action potentials and a Hamming window was applied to the band-pass signal. Evaluations of the HFO spectral frequency distribution and groupings of HFO into ripple and FR frequency ranges were based on the results of nonlinear curve-fitting analysis (GraphPad Software, San Diego, CA). "Best-fit" of nonlinear models to the data, in our case the Lorentzian, was determined from the results of the *F* test between pairs of models. The Lorentzian distribution can be described by the formula $Y = (X)/\{1 + [(X - m)/w]^2\}$, where m equals the median of the distribution and w equals the width of the distribution at half its maximal height. Confidence limits were derived from the equation $P(X) = (1/\pi) \times \{(w/2)/[(X - m)^2 + (w/2)^2]\}$.

In addition to calculating the rate of FR and ripple discharge per recording site, we calculated the ratio of FR to ripple rates as a measure of the predominant type of oscillatory event associated with each recording site. Ratio values were transformed to a logarithmic scale such that ratio values greater than 0 would reflect sites with higher rates of FR discharge compared with rates of ripple discharge. Conversely, ratio values less than 0 would reflect sites with lower rates of FR discharge compared with rates of ripple discharge. Ratio values equal to 0 would indicate sites that had equivalent rates of FR and ripple discharge. Statistical analyses of HFO peak spectral frequency and duration distributions were made with Mann-Whitney *U* test and Kruskal-Wallis tests. A factorial ANOVA model was used to compare FR and ripple rates of occurrence and ratio of FR to ripples in relation to side of seizure onset (ipsilateral vs. contralateral), anatomical recording site (Hip vs. EC), and MRI finding of Hip atrophy (presence vs. absence of atrophy). Post hoc comparisons were made using Bonferroni corrected *t*-tests. All data sets were tested for normality prior to evaluation with parametric tests using Kolmogorov-Smirnov test. Square-root transformations were employed for evaluation of non-normal distributions. Statistical significance was set at $P \leq .05$ for all analyses.

RESULTS

Sixty-four recording sites in 25 epileptic patients were analyzed for the presence of HFO activity during polysomnographically staged episodes of NREM sleep. Table 1 shows the breakdown of the recording sites separated by anatomical location and in relation to areas of seizure onset. The mean length of time analyzed per site was 177 ± 7 (SE) min. There was no difference in the amount of EEG data analyzed between sites ipsilateral to seizure onset and contralateral sites on a minutes per site basis (176 ± 10 vs. 177 ± 9 min; $t = 0.27$, df. = 62, $P = 0.7$) nor was there a significant difference on a minutes per patient basis (226 ± 22 vs. 177 ± 27 min; $t = 1.54$, df. = 24, $P = 0.1$)

Of the 64 recording sites analyzed, 38 sites were ipsilateral to areas of seizure initiation, while 26 were located contralateral to areas of seizure onset. Of the 38 sties ipsilateral to seizure onset, evaluation of MRI scans revealed atrophy in 18 sites, while the remaining 20 sites had no detectable atrophy. Of the 26 sites contralateral to seizure onset, 14 sites were contralateral to atrophy, and in the remaining 12 sites, no atrophy was detected.

Overall, high-frequency oscillations were detected in 47 of the 64 sites representing 23 patients (Table 1). In two patients, HFO activity was not detected. A greater percentage of Hip sites ipsilateral to seizure onset were identified with HFO activity compared with Hip sites contralateral to seizure onset (18 of 20 ipsilateral vs. 9 of 16 contralateral, Fisher's exact test, $P = 0.04$). No difference was found between the percent-

TABLE 1. *Mesial temporal lobe recording sites*

	Total	Ipsilateral	Contralateral
Sites	64 (25)	38 (22)	26 (17)
Sites w/ HFOs	47 (23)	32 (19)	15 (13)
Rec. time/site	177 ± 7	176 ± 10	177 ± 9
Hip			
Sites	36 (22)	20 (19)	16 (14)
Sites w/ HFOs	27 (19)	18 (18)*	9 (9)
EC			
Sites	28 (21)	18 (15)	10 (8)
Sites w/ HFOs	20 (18)	14 (14)	6 (6)

Total number of recording site analyzed, number of sites that detected high-frequency oscillation (HFO) activity, and mean ± SE length of recording per site in minutes ("Rec. time/site"). Totals shown in relation to side of seizure onset (ipsilateral vs. contralateral) and anatomical location [hippocampal vs. entorhinal cortex (Hip vs. EC)]. Number of patients represented in each category indicated in parentheses. Number of Hip sites ipsilateral to seizure onset that detected HFOs was greater compared to number of contralateral Hip sites (* $P = 0.04$).

age of EC sites ipsilateral to seizure onset where HFOs were recorded compared with the number of contralateral EC sites ($P = 0.4$). Comparisons between Hip and EC sites revealed no difference between the percentage of ipsilateral Hip sites with HFOs compared with percentage of ipsilateral EC sites with HFOs ($P = 0.4$). Similarly, no difference was found between the percentage of contralateral Hip sites with HFOs and the percentage of contralateral EC sites with HFOs ($P = 1$).

Characteristics of HFO

Figure 2 contains examples of HFOs that were detected from microelectrodes within the Hip and EC of epileptic patients, using a 5 SD RMS threshold as described in METHODS and illustrated in Fig. 1. Power spectral analysis of the three detected HFOs in this figure revealed peaks in the PSD histogram between 80 and 500 Hz. Inspection of PSD histograms, like the one in Fig. 2*B*, typically revealed a narrow peak in power at frequencies ranging between 80 and 150 Hz. A broader peak in power was commonly observed at frequencies greater than 200 Hz, for example Fig. 2*A*. The sensitivity of the power spectral analysis to accurately reflect changes in HFO frequency is illustrated in Fig. 2*C*. The first 30 ms of the event begins as a low-frequency oscillation (approximately 90 Hz) that is immediately followed (within 10 ms) by a much higher frequency oscillation (approximately 370 Hz). Inspection of a sample of PSD histograms ($n = 200$) revealed that bimodal PSDs within the same event, like that shown In Fig. 2*C*, represented <5% of those events detected.

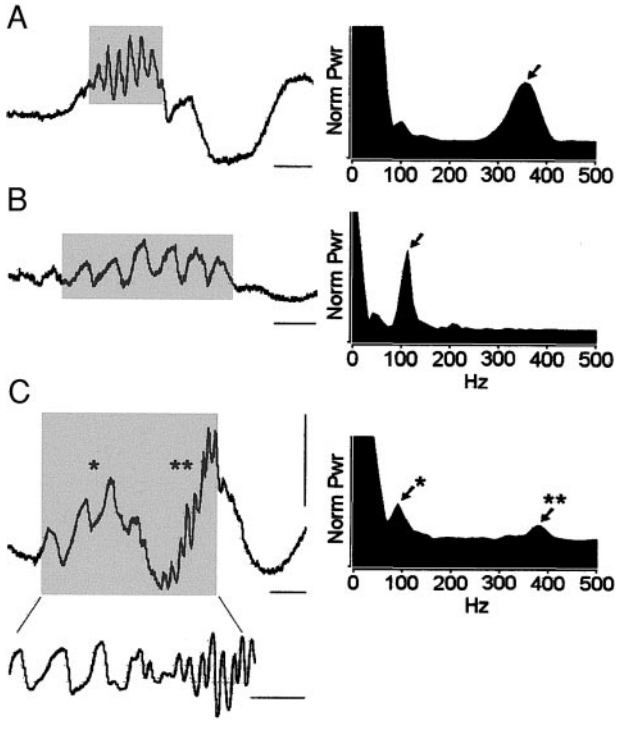

FIG. 2. HFOs and power spectral analysis. *Left*: wideband EEG traces and corresponding power spectral density histograms (*right*) illustrate 3 examples of HFOs recorded in hippocampal (Hip) and entorhinal cortical (EC) areas. ▨, segments of wideband EEG that represent HFOs detected using criteria described in METHODS and used in the power spectral analysis. *A*: HFO recorded from *patient 318* within Hip ipsilateral to site of seizure onset. Power spectral analysis reveals peak spectral frequency at 350 Hz (↓). *B*: lower-frequency HFO (110 Hz) recorded within Hip of *patient 339.* Hip recording site was contralateral to site of seizure onset. *C*: HFO recorded from EC contralateral to seizure onset of *patient 318.* Note how the first 30 ms of the HFO begins as a low frequency oscillation (90 Hz; *) that changes to a much higher frequency oscillation (370 Hz: **). ▨, segment of EEG that was band-pass filtered 80–500 Hz and the gain increased 2 times for clarity of illustration. Calibration bars 0.5 mV for all panels and 5, 10, and 15 ms for *A–C*, respectively.

Figure 3, *A* and *B*, illustrates averaged waveforms ($n = 60$) and corresponding averaged PSD histograms of representative HFOs detected in two different patients. Variability in the averaged waveform and peak spectral power, indicated by gray shading in Fig. 3, *A* and *B*, was reduced among HFOs with frequencies between 80 and 150 Hz (Fig. 3*A*) compared with the variability associated with HFOs greater than 200 Hz (Fig. 3*B*). Preliminary results of power spectral analysis and inspection of waveform morphology did not reveal any difference between HFOs recorded in Hip sites compared with EC sites. For this reason, HFOs recorded from Hip and EC sites were combined for analysis.

From 47 sites (see Table 1), 5,789 HFOs were detected during episodes of polysomnographically staged NREM sleep. Figure 4*A* shows the distribution of the peak spectral frequencies for all HFOs detected during NREM sleep. Inspection of the distribution reveals a narrow peak at the low end of the 80- to 500-Hz frequency range bounded on the left by the frequency cutoff at 80 Hz. Although there were no filter limits to the right of the peak, the number of oscillatory events dropped sharply to a minimum at about 150 Hz, followed by another peak that was much broader and centered at 270 Hz.

To determine whether the bimodal spectral frequency distribution represented two spectrally distinct groups of HFOs, we used nonlinear curve-fitting analysis to evaluate the HFO distribution. Figure 4*A* shows that the HFO spectral frequency distribution could be described as the sum of two Lorentzian distributions [results of curve-fitting denoted by dashed line; see METHODS for calculation]. Similar to the Gaussian or normal distribution, the Lorentzian distribution has a central midpoint, in this case the median, and width that reflects the dispersion surrounding the median. The parameters describing the two groups in the sample of HFO events shown in Fig. 4*A* were as follows: the lower frequency HFO group had a median frequency of 96 Hz and width of 14 Hz, while the higher-frequency group had a median and width of 262 and 59 Hz, respectively. Results of the "goodness of fit" of the curve to observed values were $R^2 = 0.94$ (df. = 25) and analysis of the residuals revealed a Kolmogorov-Smirnov distance of 0.22 ($P > 0.10$), indicating the residuals were normally distributed. Calculation of upper and lower 99% confidence limits for the two groups were 50–140 Hz for the lower-frequency group and 170–355 Hz for the higher-frequency group.

These results indicate that there are two groups of oscillations with nonoverlapping frequency ranges in this sample of HFOs. The lower-frequency group of HFOs falls within the frequency range corresponding to ripple oscillations recorded in non-primate and human Hip-EC areas (Bragin et al. 1999a; Buzsaki et al. 1992; Ylinen et al. 1995). Based on these findings and the limits of the confidence interval, we grouped HFOs between 80 (our lower cutoff limit) and 140 Hz and labeled them ripples. Likewise, the range of frequencies ascribed to pathological FR oscillations that have been reported in epileptic rodents and humans (Bragin et al. 1999a–c) overlaps with the higher-frequency HFO group. For this reason, and based on the confidence limits for the higher-frequency HFO

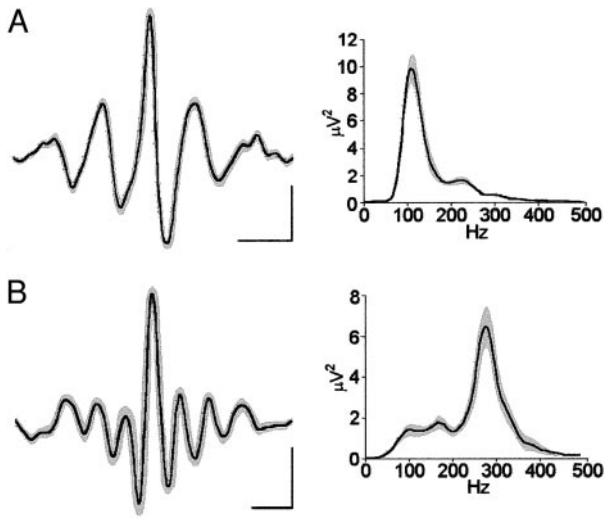

FIG. 3. HFO waveform and spectral frequency variability. *A* and *B*: averaged waveforms (*left*, both panels: $n = 60$ events) recorded from Hip sites ipsilateral to seizure onset in 2 different patients. Averaged waveforms were derived from oscillations detected using the techniques described in METHODS and aligned on the maximum positive peak of the oscillatory event. Gray shading surrounding averaged waveforms and averaged PSD histograms (*right*) represent standard errors. Note the reduced variability of both the waveform and spectral frequency for the lower-frequency events (*A*) compared with the higher-frequency events (*B*). Power spectra calculations in *A* and *B* performed on events band-pass filtered (80–500 Hz) to reduce the power associated with slow waves contributing to the power spectra. Calibration bars 100 μV for both panels and 10 and 5 ms for *A* and *B*, respectively.

group, HFOs greater than 170 Hz were combined and labeled FR. Due to the equivocal association of HFOs within the range of 141–169 Hz with either FR or ripples, we excluded HFO events ($n = 278$) within this frequency range to better contrast the two groups of HFOs.

Figure 4, *B* and *C*, shows the number of ripples and FR that were recorded in relation to area of seizure onset. The number of ripples and FR detected from sites contralateral to seizure onset were 1,868 and 398, respectively (Fig. 4*B*). In contrast, Fig. 4*C* shows that fewer ripples ($n = 1{,}342$) and a greater number of FR ($n = 1{,}903$) were detected from sites ipsilateral to seizure onset. Comparing the total number of ripples and FR detected in relation to side of seizure onset, χ^2 analysis revealed that the relative number of ripples to FR that were detected was strongly associated with side of seizure onset ($\chi^2 = 924$, $P < 0.0001$).

Figure 5 shows the distribution of FR and ripple durations for all events recorded ipsilateral and contralateral to seizure onset. In spite of the overlap in the distributions of FR and ripple durations, overall, FR were shorter in duration than ripples (Mann-Whitney, $P < 0.0001$). The median duration for FR was 15.2 ms and 25th to and 75th percentiles were 12.7 and 19.1, ms, respectively. In comparison, the median ripple duration was 32.4 ms and 25th and 75th percentiles were 26.1 and 40.2 ms, respectively. Interestingly, analysis of the durations of FR detected in relation to side of seizure onset revealed that FR detected ipsilateral to areas of seizure onset were shorter in duration compared with FR detected in areas contralateral to seizure onset (14.7 vs. 18.1 ms; $P < 0.0001$). Similarly, the median duration of ripples detected ipsilateral to seizure onset was shorter compared with the duration of ripples detected contralateral to seizure onset (28.9 vs. 34.6 ms; $P < 0.0001$). Correlation analysis between HFO duration and peak spectral frequency also showed that duration was negatively correlated with spectral frequency (Spearman rank test, $\rho = -0.7$, $P < 0.0001$).

FR and ripples in relation to areas of seizure onset

Of the 32 sites ipsilateral and 15 sites contralateral to seizure onset that showed evidence of oscillatory activity, FR were detected in 32 of 32 ipsilateral sites and 12 of the 15 contralateral sites. Ripples were detected in 28 of the 32 ipsilateral sites

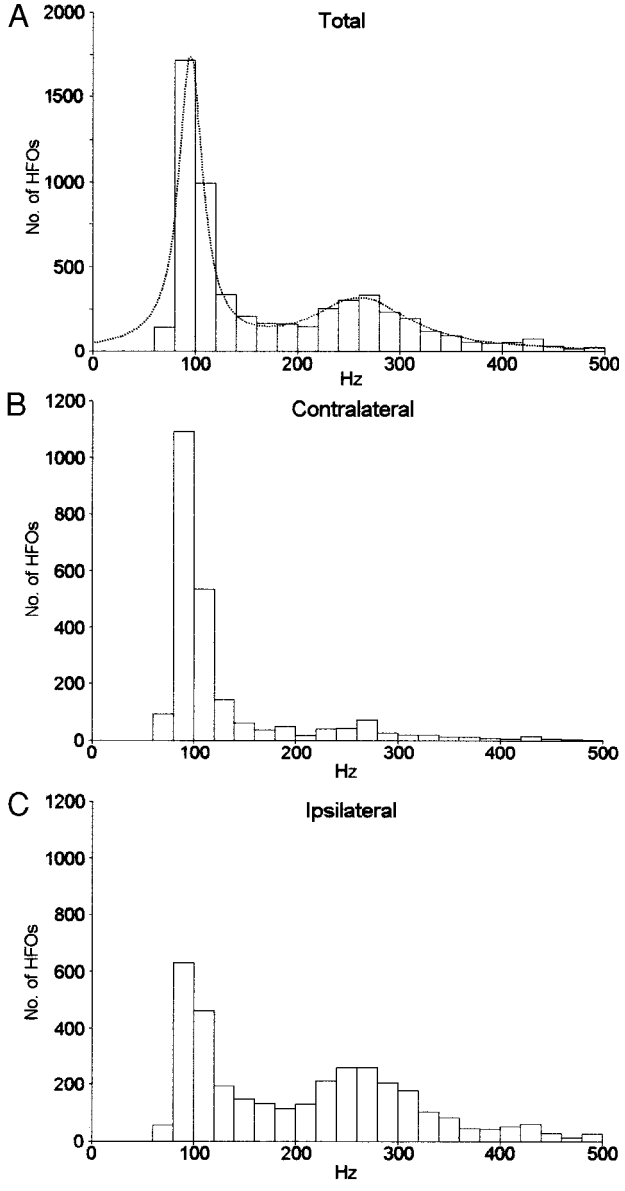

FIG. 4. Distribution of HFOs peak spectral frequencies. *A*: total number of HFOs detected from 25 patients during non-rapid eye-movement (NREM) episodes. - - -, results of curve-fitting analysis that revealed the distribution could be described by the sum of 2 Lorentzian distributions. Note the narrow peak within the distribution centered at 96 Hz and broader peak centered at 260 Hz. *B* and *C*: number of HFOs detected in relation to side of seizure onset. A greater number of ripple oscillations (80–140 Hz) were found in sites contralateral to areas of seizure onset (*B*). In contrast, more fast ripple (FR) oscillations (170–500 Hz) were recorded in sites ipsilateral to seizure onset (*C*). Bin width for all histograms 20 Hz.

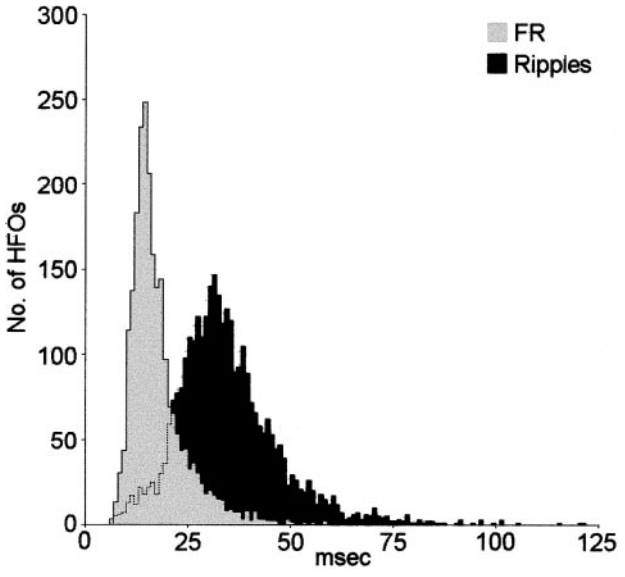

FIG. 5. Distribution of ripple and FR durations. Note the separation in distributions between the shorter duration FR frequency oscillations (▨) compared with relatively longer duration ripple frequency oscillations (■). FR were significantly shorter in duration compared with ripples. Bin width: 1 ms.

and in 15 of 15 contralateral sites. Figure 6*A* shows that the mean rate of FR discharge per 10-min NREM episode was 3.33 ± 0.63 in areas ipsilateral to seizure onset compared 1.22 ± 0.71 in areas contralateral to seizure onset. In spite of mean FR rates more than 2.5 times greater ipsilateral to seizure onset compared with contralateral, these differences were not significant [ANOVA, $F(1,43) = 2.54$, $P = 0.1$]. No difference in FR rates were found between Hip and EC [$F(1,43) = 0.01$, $P = 0.9$; Hip, 2.26 ± 0.63 vs. EC, 3.21 ± 1.22] or between Hip and EC sites in relation to side of seizure onset [$F(1,39) = 2.84$, $P = 0.1$]. Examination of the influence of MRI-defined Hip atrophy on FR rates in relation to side of seizure onset revealed a trend toward higher FR rates in areas ipsilateral to both seizure onset and atrophy compared with FR rates in sites contralateral to both seizure onset and atrophy, but differences were not significant [$F(1,43) = 3.25$, $P = 0.07$]. In contrast, Fig. 6*B* reveals that the rate of occurrence of ripples per 10 min NREM episode was less in areas ipsilateral to seizure onset (2.66 ± 1.2) compared with areas contralateral to seizure onset (5.86 ± 3.8), but differences in mean ripple rates between ipsilateral and contralateral sites were not significant [$F(1,43) = 0.49$, $P = 0.4$]. Similarly, no difference in rate was found between Hip and EC sites [$F(1,43) = 3.01$, $P = 0.09$; Hip 4.79 ± 2.5 vs. EC, 2.18 ± 0.92] or between Hip and EC sites in relation to seizure onset [$F(1,43) = 1.04$, $P = 0.3$]. The effects of Hip atrophy on ripple rates in relation to side of seizure onset were not significant [$F(1,43) = 2.05$, $P = 0.1$].

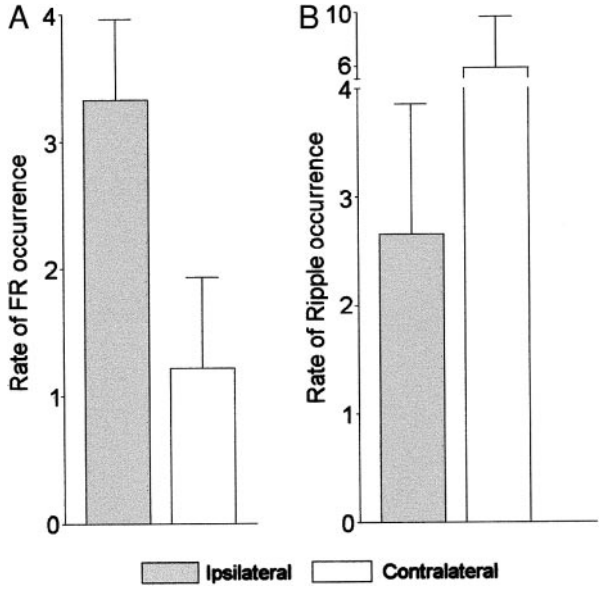

FIG. 6. Mean rate of FR and ripple occurrence per 10-min period. *A*: FR occurred an average 2.5 times more frequently in areas ipsilateral to seizure onset compared with contralateral sites. In spite of these differences in mean rate of discharge, rates of FR discharge were not statistically significant ($P = 0.1$). *B*: ripples occurred less frequently in areas ipsilateral to seizure onset compared with contralateral sites. Note the break in the ordinate scale and change in scaling factor to accommodate for the higher rate of ripple occurrence in sites contralateral to seizure onset. Error bars reflect the SE.

Figure 7 shows the mean ratio of FR to ripple discharge in sites ipsilateral to seizure onset compared with the ratio of FR to ripple discharge in sites contralateral to seizure onset. Ratio values greater than 0 reflect a higher rate of FR discharge relative to ripple discharge, while values less than 0 reflect a lower rate of FR discharge relative to the rate of ripple discharge. The bars labeled "total" in Fig. 7 show that the mean ratio ipsilateral to seizure onset was greater compared with the ratio contralateral to seizure onset. This difference was highly significant [$F(1,39) = 9.85$, $P = 0.003$]. The mean ± SE ratios for sites ipsilateral compared with sites contralateral to seizure onset were 0.36 ± 0.16 versus −0.37 ± 0.23 ($P = 0.008$). Consistent with the rate analyses, comparison of ratios between

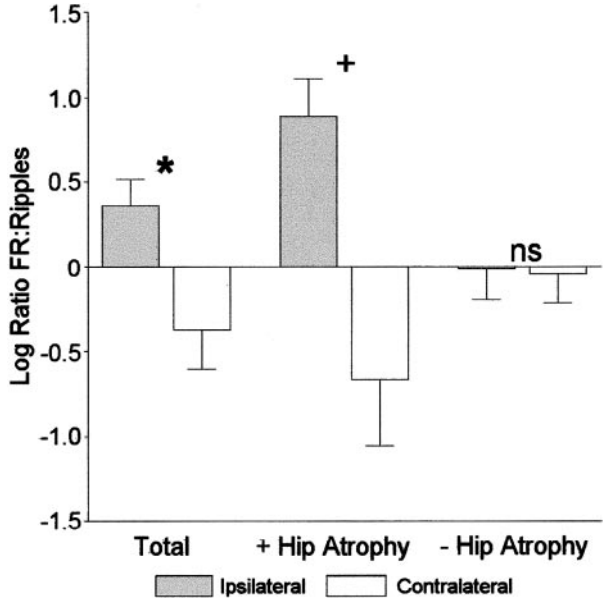

FIG. 7. Ratio of FR to ripple generation recorded ipsilateral and contralateral to seizure onsets. Logarithmic values greater than 0 reflect a greater number of FR relative to ripples, while a values less than 0 reflect fewer FR relative to ripples. Mean ± SE ratio from recording sites ipsilateral seizure onset ("Total") was significantly greater compared sites contralateral to seizure onset. Analysis of recording sites that were ipsilateral to both seizure onset, and MRI defined Hip atrophy ("+ Hip Atrophy") revealed a significantly higher ratio of FR to ripples compared with sites contralateral to both seizure onset and Hip atrophy. No difference in mean ratios was observed between sites ipsilateral to seizure onset without Hip atrophy ("− Hip Atrophy") and contralateral to seizure onset without Hip atrophy. * $P = 0.008$; + $P = 0.001$

Hip and EC did not reveal any difference [$F(1,39) = 0.0001$, $P = 0.9$] or between Hip and EC sites in relation to side of seizure onset [$F(1,39) = 0.11$, $P = 0.7$].

Further examination of the ratio results revealed that incorporation of MRI findings for the presence or absence of Hip atrophy were useful in identifying recording sites contributing most heavily to differences in the mean ratios [$F(1,39) = 8.28$, $P = 0.006$). Figure 7 (bars labeled "+ Hip Atrophy") shows that sites that were ipsilateral to both seizure onset and Hip atrophy had a significantly higher mean ratio compared with sites that were contralateral to both seizure onset and Hip atrophy (0.89 ± 0.22 vs. -0.66 ± 0.39; $P = 0.001$). Conversely, no difference in mean ratio was found between sites ipsilateral to seizure onset without Hip atrophy (Fig. 7, bars labeled "–Hip Atrophy") compared with sites contralateral to seizure onset without Hip atrophy (-0.01 ± 0.18 vs. -0.04 ± 0.17; $P = 0.9$).

DISCUSSION

In the present study, spectral frequency analysis of interictal wideband EEG activity has provided new quantitative evidence describing the distribution and prevalence of ripple and FR frequency oscillations in the epileptic human Hip and EC. These data show that the ratio of FR to ripple generation is significantly greater at sites ipsilateral to seizure onset compared with the ratio of FR to ripples at sites contralateral to seizure initiation. Moreover, the presence of Hip atrophy was found to be a significant factor in creating the higher relative rate of FR in epileptogenic regions. These findings further substantiate the value of HFO activity as a marker of epileptogenicity in the human epileptic temporal lobe.

Ripple and FR oscillations

Ripple oscillations (100–200 Hz) are generated chiefly during slow-wave sleep and waking immobility and have been recorded within area CA1 of hippocampus, subiculum, and entorhinal cortex of nonepileptic rodents (Buzsaki et al. 1992; Chrobak and Buzsaki 1996; Ylinen et al. 1995). Buzsaki and colleagues have also shown that ripple oscillations in CA1 pyramidal cells are dependent on synchronous GABAergic interneuron discharge. In addition to their appearance in nonepileptic rodents, ripples remain present in Hip and EC areas of rodents made epileptic and are found both ipsilateral and contralateral to the lesioned area (Bragin et al. 1999b). Evidence of ripple frequency oscillations within humans has been provided in studies recording from Hip and EC of epileptic patients (Bragin et al. 1999a,b). While sharing many characteristics of non-primate ripples, i.e., behavioral state, anatomical location, rate of occurrence, it was reported that human ripples were of a slightly lower frequency (80–160 Hz).

In contrast to ripple oscillations, FR were first described in studies of the intrahippocampal kainic-acid-injected rodent model of epilepsy and later found in the Hip and EC of epileptic patients. In both, FR displayed a higher spectral frequency (250–500 Hz) compared with ripples, and in both, FR were observed only in Hip and EC areas ipsilateral to the lesioned site of the epileptic brain (Bragin et al. 1999a–c). Equally important, in control animals from the studies cited in the preceding text, FR were not detected in either Hip or EC areas. Furthermore, FR were found in dentate gyrus of the epileptic rodent (Bragin et al. 1999a), an area in which ripples have not been recorded in the nonepileptic brain. Consistent with the preceding evidence supporting the existence of two unique oscillatory events, in the present study, based on curve-fitting of the frequency distribution of a large sample of these events (Fig. 4), we provide evidence for human ripple frequency oscillations that, using these quantitative techniques, were found to extend from 80 to 140 Hz, and FR frequency oscillations extending greater than 170 Hz, and up to 500 Hz. Qualitatively, we show that the variability among FR frequency oscillations was greater compared with ripple frequency oscillations; this may be related to the disparate frequency ranges associated with these two oscillatory events.

Differences in ripple and FR frequencies between this study and earlier human studies may be due to the substantially larger sample of ripples and FR and differences in methods of event detection. It should be noted that the spectral frequency distribution bounded on the left by our 80-Hz cutoff frequency may have contributed to the decreased variability among ripples, thus constricting the frequency limits associated with ripple oscillations that may have excluded ripple oscillations greater than 140 Hz. In addition, quantification of the power spectral analysis may account for the slightly lower ripple and FR frequencies found in this study. However, in studies of the rodent hippocampal CA3 area, power spectral analysis has been successfully used to differentiate small-amplitude ripple oscillations between 100 and 130 Hz from large-amplitude ripples between 140 and 200 Hz recorded in CA1 areas (Buzsaki et al. 1992; Csicsvari et al. 1999).

In addition to the spectral frequency differences between FR and ripples, we found FR to be shorter in duration compared with ripples. The durations of ripples and FR detected in our study are generally consistent with those previously reported in rodents and humans (Bragin et al. 1999a; Buzsaki et al. 1992). Our analyses revealed that FR recorded ipsilateral to seizure onsets were of significantly shorter duration than FR recorded from contralateral sites. Likewise, ripples recorded ipsilateral to seizure onsets were of shorter duration than ripples recorded from contralateral sites. These results suggest more powerful synchronization of cellular events underlying ripple and FR generation, which is then followed by strong suppression of neuronal discharge. If the suppression is due to inhibition, the short-duration of FR may be $GABA_A$ receptor mediated. Recent evidence by Jones and Barth (2002) shows that fast neocortical oscillations increased in duration after epicortical application of the $GABA_A$ receptor antagonist, bicuculline, during the development of epileptogenesis, and application of bicuculline to hippocampal slices from rats with chronic seizures has been shown to prolong the duration and increase the spatial extent of evoked FR (Bragin et al. 2002). Moreover, sprouting of GAD-positive terminals has been observed in sclerotic hippocampi (Babb et al. 1989; Davenport et al. 1990), and there is evidence of functional inhibition in epileptogenic-seizure-generating areas (Swanson et al. 1998; Wilson et al. 1998), both suggesting the continued presence of robust inhibitory mechanisms that can dampen hypersynchronous oscillatory bursts in seizure generating areas. In addition, transitory hypersynchronization of neuronal activity hypothesized to occur during FR generation within seizure initiating areas (Bragin et al. 2002) is consistent with our single-neuron studies that

found significantly higher burst rates, shorter-duration action potential bursts, and greater synchrony of discharge of single neurons in areas ipsilateral to seizure onsets compared with single neurons contralateral to seizure onset (Staba et al. 2002).

Ripples, FR, and epileptogenicity

The proposal that FR reflect the hypersynchronous activity within epileptogenic regions capable of generating seizures derives from studies showing FR were limited to areas ipsilateral to the lesioned site in epileptic rodents (Bragin et al. 1999b) and epileptic patients (Bragin et al. 1999a). Consistent with earlier studies, the present study found that the proportion of FR to ripples was significantly associated with side of seizure onset. However, our technique also detected FR in contralateral mesial temporal lobe sites, sites where FR were not detected in previous studies of epileptic animals and patients (Bragin et al. 1999a,b). One reason for this may be the extended periods of recordings used in this study compared with previous studies that may have increased the likelihood of detecting FR which were occurring only at very rare intervals (rate of 0.1/10 min). Furthermore, our analyses were limited to polysomnographically defined episodes of NREM sleep compared with previous analyses that were performed while patients were awake or drowsy (Bragin et al. 1999a,b). The greater degree of neuronal synchronization associated with deeper stages of NREM sleep may have also increased the probability that our automated technique would detect any occurrence of FR. It has long been known that epileptiform interictal spikes are most widely distributed and least useful for epileptogenic localization during NREM sleep (e.g., Lieb et al. 1980). Finally, it is also known that spontaneous seizures may arise independently from both hippocampi in patients with mesial temporal lobe epilepsy (Engel et al. 1997), and our ability to detect FR in sites contralateral to seizure onset may reflect secondary epileptogenic areas in the opposite hemisphere that are capable of independently, albeit infrequently, generating seizures.

Although a greater number of FR and fewer number of ripples was clearly associated with areas of seizure genesis, individual analysis of the rate of FR and ripple occurrence did not reveal statistical differences for either FR or ripples in relation to side of seizure onset. One factor that may have contributed to the rate differences between human and animal studies may be due to the use of fixed microelectrodes in patient recordings, and moveable microelectrodes in animal recordings. Previous studies in rodents have shown that the probability of detecting FR with fixed electrodes was lower compared with moveable electrodes (Bragin et al. 2002). Based on the evidence suggesting larger networks underlie ripple generation (Chrobak and Buzsaki 1996) compared with networks governing FR generation (Bragin et al. 2002), the localization of sites with high FR rates may have been compromised because the fixed electrodes were not in optimal locations to detect the smaller network generated FR oscillations.

Results from the analyses comparing the ratio of FR to ripple discharge in relation to side of seizure onset revealed that greater rates of FR discharge and lower rates of ripple discharge characterized sites ipsilateral to seizure onset compared with the lower rates of FR and higher rates of ripple discharge in contralateral sites. Moreover, ratios of FR to ripple discharge were significantly greater from sites ipsilateral to seizure onset in which Hip atrophy was detected, compared with sites contralateral to both seizure onset and Hip atrophy. In vivo (Bragin et al. 2002; Buckmaster and Dudek 1997) and in vitro (Patrylo et al. 1999; Wuarin and Dudek 1996) stimulation studies recording from hippocampal areas of kainate-treated rats have shown that areas of dentate gyrus with pronounced cell loss and aberrant synaptic reorganization generate hypersynchronous epileptiform and seizure-like activity. Histological analysis of surgically resected human epileptogenic tissue has found significant changes in the cellular substrate of both epileptic Hip (Babb and Brown 1987; de Lanerolle 1989; Houser et al. 1990; Sutula et al. 1989) and epileptic EC (Bothwell et al. 2001; Du et al. 1993), suggesting that alterations in local circuitry may be associated with seizure genesis. Furthermore, the evidence of mossy fiber sprouting observed in the studies cited in the preceding text and sprouting of GABAergic axons (Babb et al. 1989; Davenport et al. 1990; Prince and Jacobs 1998), which may contribute to the enhanced paired-pulse inhibition found in seizure generating areas (Wilson et al. 1998), suggests that aberrant excitatory and inhibitory connections may underlie the hypersynchronous activity within seizure generating areas. In a previous study, we found single neurons in areas ipsilateral to seizure onset had higher burst rates and greater synchrony of discharges compared with neurons in contralateral areas (Staba et al. 2002). The overall reduction in the number of ripples in areas ipsilateral to seizure onset compared with the number of ripples detected in contralateral areas may be due to oscillatory events that begin as ripple oscillations, but due to alterations in local circuitry, transition to hypersynchronous FR oscillations (see Fig. 2*C*). However, because we estimated that such events amounted to less than 5% of the total events detected, this alone would not account for the difference in ripples between ipsilateral and contralateral areas. Finally, as proposed by Bragin and colleagues (2000), FR within seizure generating areas are thought to reflect the hypersynchronous neuronal discharge of aberrantly interconnected clusters of neurons, possibly mediated by axoaxonal gap junctions, local disturbances in inhibition, or strengthened local excitatory connections. If the latter, areas with higher ratios of FR to ripples may reflect an increase in the density of aberrant excitatory connections between surviving principle cells.

In evaluating these data, one must consider that contralateral sites were defined on the basis of electrographic data acquired during the average 2 wk of depth electrode monitoring as areas where seizure initiation was not observed. However, it is possible that seizures may have arisen from contralateral areas in prior years during the course of epileptogenesis. Likewise, in the years after epilepsy surgery, if it was observed that in some patients seizure control was not obtained from removal of ipsilateral areas, we may have incorrectly classified some FR oscillations. Alternatively, subtle asymmetries between hippocampi that are associated with pathology may have gone undetected during inspection of MRI scans. Incorporating data from MRI volumetry studies, PET imaging, histological analysis, and patient surgical outcomes with the present results should provide additional information that will help characterize ripple and FR activity in areas of greater and lesser seizure generating potential and assist in understanding the contrast between the occurrence of FR in human epileptogenesis and

the presence of FR activity in animal models of chronic epilepsy.

Localization significance of ripple and FR oscillations

The presence of FR oscillations in the epileptic EEG has not been previously recognized because of the bandwidth limitations of most of the clinical EEG monitoring systems now in use. It is possible that both a reduction in discharge of ripples and an increase in discharge of FR may provide additional localizing information during diagnostic recordings of interictal wideband EEG in patients requiring seizure-localization studies. The sensitivity of FR generation as a marker of epileptogenicity is currently under investigation by comparing how neuromodulatory changes associated with changes in brain state, i.e., wakefulness and sleep, influence FR generation.

The authors thank J. Herrmann, D. Jhung, and N. Redjal for assistance with data processing and T. Fields and E. Behnke for excellent technical assistance.

This work was sponsored by National Institute of Neurological Disorders and Stroke, Grants NS-02808 and NS-33310.

REFERENCES

AMARAL D AND INSAUSTI R. *The Human Nervous System.* San Diego, CA: Academic,1990, p. 711–755.

BABB TL AND BROWN WJ. *Surgical Treatment of the Epilepsies.* New York: Raven, 1987, p. 511–540.

BABB TL, PRETORIUS JK, KUPFER WR, AND CRANDALL PH. Glutamate decarboxylase-immunoreactive neurons are preserved in human epileptic hippocampus. *J Neurosci* 9: 2562–2574, 1989.

BOTHWELL S, MEREDITH GE, PHILLIPS J, STAUTON H, DOHERTY C, GRIGORENKO E, GLAZIER S, DEADWYLER SA, O'DONOVAN CA, AND FARRELL M. Neuronal hypertrophy in the neocortex of patients with temporal lobe epilepsy. *J Neurosci* 21: 4789–4800, 2001.

BRAGIN A, ENGEL J JR, WILSON CL, FRIED I, AND BUZSAKI G. High-frequency oscillations in human brain. *Hippocampus* 9: 137–142, 1999a.

BRAGIN A, ENGEL J JR, WILSON CL, FRIED I, AND MATHERN GW. Hippocampal and entorhinal cortex high-frequency oscillations (100–500 Hz) in human epileptic brain and in kainic acid-treated rats with chronic seizures. *Epilepsia* 40: 127–137, 1999b.

BRAGIN A, ENGEL J JR, WILSON CL, VIZENTIN E, AND MATHERN GW. Electrophysiologic analysis of a chronic seizure model after unilateral hippocampal KA injection. *Epilepsia* 40: 1210–1221, 1999c.

BRAGIN A, MODY I, WILSON CL, AND ENGEL J JR. Local generation of fast ripples in epileptic brain. *J Neurosci* 22: 2012–2021, 2002.

BRAGIN A, WILSON CL, AND ENGEL J JR. Chronic epileptogenesis requires development of a network of pathologically interconnected neuron clusters: a hypothesis. *Epilepsia* 41: S144–S152, 2000.

BRAGIN A, WILSON CL, STABA RJ, REDDICK M, FRIED I, AND ENGEL J JR. Interictal high-frequency oscillations (80–500 Hz) in the human epileptic brain: entorhinal cortex. *Ann Neurol* In press.

BUCKMASTER PS AND DUDEK FE. Network properties of the dentate gyrus in epileptic rats with hilar neuron loss and granule cell axon reorganization. *J Neurophysiol* 77: 2685–2696, 1997.

BUZSAKI G. Memory consolidation during sleep: a neurophysiological perspective. *J Sleep Res* 7: 17–23, 1998.

BUZSAKI G, HORVATH Z, URIOSTE R, HETKE J, AND WISE K. High-frequency network oscillation in the hippocampus. *Science* 256: 1025–1027, 1992.

CHROBAK JJ AND BUZSAKI G. High-frequency oscillations in the output of the hippocampal-entorhinal axis of the freely behaving rat. *J Neurosci* 16: 3056–3066, 1996.

CSICSVARI J, HIRASE H, CZURKO A, MAMIYA A, AND BUZSAKI G. Fast network oscillations in the hippocampal CA1 region of the behaving rat. *J Neurosci* 19: 1–4, 1999.

CURIO G, MACKERT BM, BURGHOFF M, KOETITZ R, ABRAHAM-FUCHS K, AND HARER W. Localization of evoked neuromagnetic 600-Hz activity in the cerebral somatosensory system. *Electroencephalogr Clin Neurophysiol* 91: 483–487, 1994.

DAVENPORT CJ, BROWN WJ, AND BABB TL. Sprouting of GABAergic and mossy fiber axons in dentate gyrus following intrahippocampal kainate in the rat. *Exp Neurol* 109: 180–190, 1990.

DE LANEROLLE NC, KIM JH, ROBBINS RJ, AND SPENCER DD. Hippocampal interneuron loss and plasticity in human temporal lobe epilepsy. *Brain Res* 495: 387–395, 1989.

DU F, WHETSELL WO, ABOU-KHALIL B, BLUMENKOPF B, LOTHMAN EW, AND SCHWARCZ R. Preferential neuronal loss in layer III of the entorhinal cortex in patients with temporal lobe epilepsy. *Epilepsy Res* 16: 223–233, 1993.

DUVERNOY HM. *The Human Hippocampus.* New York: Springer, 1998.

ENGEL J JR. Introduction to temporal lobe epilepsy. *Epilep Res* 26: 141–150, 1996.

ENGEL J JR, WILLIAMSON PD, AND WIESER HG. Mesial temporal lobe epilepsy. *Epilepsy: A Comprehensive Textbook,* edited by Engel JJ and Pedley TA. Philadelphia, PA: Lippincott-Raven, 1997, p. 2417–2426.

FISHER RS, WEBBER WR, LESSER RP, ARROYO S, AND UEMATSU S. High-frequency EEG activity at the start of seizures. *J Clin Neurophysiol* 9: 441–448, 1992.

FRIED I, WILSON CL, MAIDMENT NT, ENGEL J JR, BEHNKE E, FIELDS TA, MACDONALD KA, MORROW JW, AND ACKERSON L. Cerebral microdialysis combined with single-neuron and electroencephalographic recording in neurosurgical patients. Technical note. *J Neurosurg* 91: 697–705, 1999.

GRENIER F, TIMOFEEV I, AND STERIADE M. Focal synchronization of ripples (80–200 Hz) in neocortex and their neuronal correlates. *J Neurophysiol* 86: 1884–1898, 2001.

HOUSER CR. Granule cell dispersion in the dentate gyrus of humans with temporal lobe epilepsy. *Brain Res* 535: 195–204, 1990.

JASPER H. Report of the committee on methods of clinical examination in electroencephalography. *Electroencephalogr Clin Neurophysiol* 10: 305–375, 1958.

JONES MS AND BARTH DS. Spatiotemporal organization of fast (>200 Hz) electrical oscillations in rat vibrissa/barrel cortex. *J Neurophysiol* 82: 1599–1609, 1999.

JONES MS, BARTH DS. Effects of bicuculline methiodide on fast (>200 Hz) electrical oscillations in rat somatosensory cortex. *J Neurophysiol* 88: 1016–1025, 2002.

JONES MS, MACDONALD KD, CHOI B, DUDEK FE, AND BARTH DS. Intracellular correlates of fast (>200 Hz) electrical oscillations in rat somatosensory cortex. *J Neurophysiol* 84: 1505–1518, 2000.

KANDEL A AND BUZSAKI G. Cellular-synaptic generation of sleep spindles, spike-and-wave discharges, and evoked thalamocortical responses in the neocortex of the rat. *J Neurosci* 17: 6783–6797, 1997.

LIEB JP, JOSEPH JP, ENGEL J JR, WALKER J, AND CRANDALL PH. Sleep state and seizure foci related to depth spike activity in patients with temporal lobe epilepsy. *Electroencephalogr Clin Neurophysiol* 49: 538–557, 1980.

O'KEEFE J AND NADEL J. *The Hippocampus As a Cognitive Map.* Oxford: Clarendon Press, 1978.

PATRYLO PR, SCHWEITZER JS, AND DUDEK FE. Abnormal responses to perforant-path stimulation in the dentate gyrus of slices from rats with kainate-induced epilepsy and mossy fiber reorganization. *Epilepsy Res* 36: 31–42, 1999.

PRINCE DA AND JACOBS K. Inhibitory function in two models of chronic epileptogenesis. *Epilepsy Res* 32: 83–92, 1998.

RECHTSCHAFFEN A AND KALES A. *A Manual of Standardized Terminology, Techniques and Scoring System for Sleep Stages of Human Subjects.* Bethesda, MD: Neurological Information Network, 1968.

ROSSI GF, COLICCHIO G, AND POLA P. Interictal epileptic activity during sleep: a stereo-EEG study in patients with partial epilepsy. *Electroencephalogr Clin Neurophysiol* 58: 97–106, 1984.

SAMMARITANO M, GIGLI GL, AND GOTMAN J. Interictal spiking during wakefulness and sleep and the localization of foci in temporal lobe epilepsy. *Neurology* 41: 290–297, 1991.

SIAPAS AG AND WILSON MA. Coordinated interactions between hippocampal ripples and cortical spindles during slow-wave sleep. *Neuron* 21: 1123–1128, 1998.

STABA RJ, WILSON CL, BRAGIN A, FRIED I, AND ENGEL J JR. Sleep states differentiate single neuron activity recorded from human epileptic hippocampus, entorhinal cortex and subiculum. *J Neurosci* 22: 5694–5704, 2002.

STABA RJ, WILSON CL, FRIED I, AND ENGEL J JR. Single-neuron burst firing in the human hippocampus during sleep. *Hippocampus* In press.

SUTULA T, CASCINO G, CAVAZOS J, PARADA I, AND RAMIREZ L. Mossy fiber synaptic reorganization in the epileptic human temporal lobe. *Ann Neurol* 26: 321–330, 1989.

SUZUKI SS AND SMITH GK. Spontaneous EEG spikes in the normal hippocampus. II. Relations to synchronous burst discharges. *Electroencephalogr Clin Neurophysiol* 69: 532–540, 1988.

SWANSON TH, SPERLING MR, AND O'CONNOR MJ. Strong paired-pulse depression of dentate granule cells in slices from patients with temporal lobe epilepsy. *J Neural Transm* 105: 613–625, 1998.

TRAUB R.D., WHITTINGTON MA, BUHL EH, LEBEAU FE, BIBBIG A, BOYD S, CROSS H, AND BALDEWEG T. A possible role for gap junctions in generation of very fast EEG oscillations preceding the onset of, and perhaps initiating, seizures. *Epilepsia* 42: 153–170, 2001.

WIESER HG. Depth recorded limbic seizures and psychopathology. *Neurosci Biobehav Rev* 7: 427–440, 1983.

WILSON CL, KHAN SU, ENGEL J JR, ISOKAWA M, BABB TL, AND BEHNKE EJ. Paired-pulse suppression and facilitation in human epileptogenic hippocampal formation. *Epilep Res* 31: 211–230, 1998.

WUARIN JP AND DUDEK FE. Electrographic seizures and new recurrent excitatory circuits in the dentate gyrus of hippocampal slices from kainate-treated epileptic rats. *J Neurosci* 16: 4436–4448, 1996.

YLINEN A, BRAGIN A, NADASDY Z, JANDO G, SZABO I, SIK A, AND BUZSAKI G. Sharp wave-associated high-frequency oscillation (200 Hz) in the intact hippocampus: network and intracellular mechanisms. *J Neurosci* 15: 30–46, 1995.